

**„BABEȘ-BOLYAI” UNIVERSITY
FACULTY OF BIOLOGY AND GEOLOGY
EXPERIMENTAL BIOLOGY DEPARTMENT**

Summary of doctoral thesis

**HEPATIC STELLATE CELLS-SPECIFIC SMAD7
EXPRESSION ATTENUATES LIVER FIBROGENESIS
IN MICE**

Ph. D student: Ph. D LOREDANA CIUCLAN

Scientific coordinator: Professor CONSTANTIN CRACIUN

**CLUJ-NAPOCA
2011**

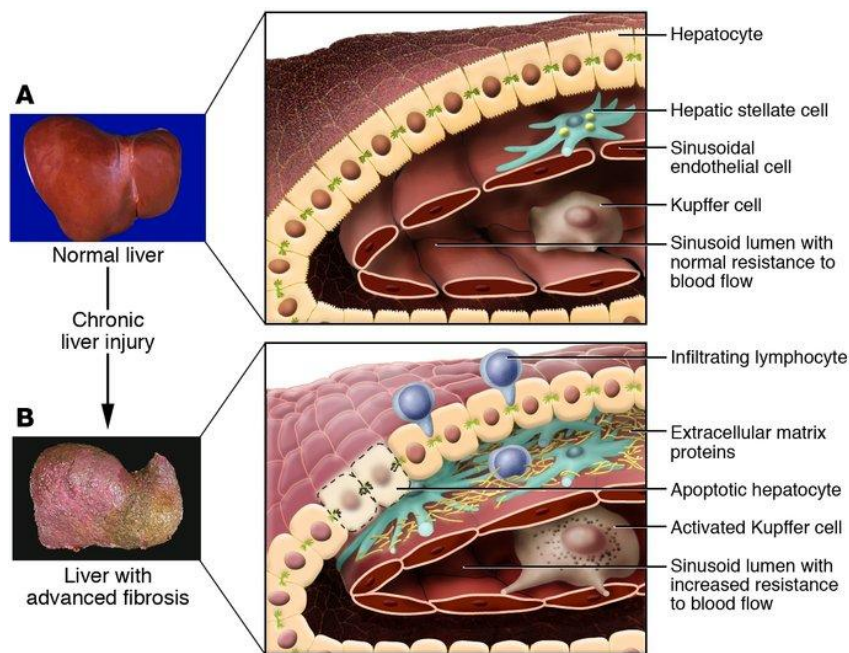
Table of Contents

| | |
|---|----|
| 1. Introduction | 3 |
| 1.1 Liver fibrosis..... | 3 |
| 1.2 Pathophysiologic Relevance of Cytokines in Chronic Liver Disease | 4 |
| 1.3 TGF- β in fibrogenesis..... | 5 |
| 1.4 TGF- β signal transduction..... | 5 |
| 1.5 Animal models for liver disease | 7 |
| 2. Aim of the study | 7 |
| 3. Materials and Methods | 8 |
| 3.1 Animals..... | 8 |
| 3.2 Establishing liver damage with bile duct ligation..... | 8 |
| 3.3 Detection of mRNA expression | 8 |
| 3.4 Immunohistochemical staining | 9 |
| 3.5 Serum Enzymes and Hepatic Fibrosis Indices | 10 |
| 3.6 Statistical analysis..... | 10 |
| 4. Results | 10 |
| 4.1 Establishing liver damage with bile duct ligation and experimental design | 10 |
| 4.2 SM22 α -Flag-Smad7 expression in FVB/N and SM22 α -Flag-Smad7 transgenic after 2 weeks of BDL.. | 11 |
| 4.3 Smad7 overexpression in HSCs decrease the serum levels of liver enzymes in BDL treated mice | 12 |
| 4.4 Smad7 overexpression in HSCs decreases collagen deposition in BDL treated mice | 14 |
| 4.5 Smad7-overexpression leads to a decrease of α -SMA synthesis in liver cells of BDL treated mice. | 15 |
| 4.6 Smad7 overexpression in HSCs blunts inflammation in BDL operated mice. | 16 |
| 4.7 Smad7 dependent gene expression pattern | 17 |
| 5. Discussion..... | 20 |
| 5.1 Myofibroblasts are the primary target of anti-fibrotic therapy | 20 |
| 5.2 The influence of Smad7, antagonist of transforming growth factor (TGF)- β canonical signaling pathways on hepatic stellate cell (HSC) transdifferentiation..... | 22 |
| 5.3 Glucose metabolism and angiogenesis/vascularisation is downregulated by Smad7 | 22 |
| 6. Conclusions | 23 |
| 7. Keywords..... | 23 |
| 8. References | 23 |

1. Introduction

1.1 Liver fibrosis

Fibroproliferative diseases are a leading cause of morbidity and mortality. Fibrosis is comparable with a wound-healing response being out of control. Repair mechanisms aim at the replacement of injured cells, however contrary to the pure regeneration of tissue in fibroplasia, connective tissue substitute normal parenchyma. The ultimate result is organ failure [8] (Fig.1).



(Modified from Brenner., 2007)

Figure.1 Sinusoidal events in the development of liver fibrosis. Injury to hepatocytes results in the recruitment and stimulation of inflammatory cells, as well as the stimulation of resident inflammatory cells (including Kupffer cells). Factors released by these inflammatory cells lead to transformation of HSCs into a myofibroblast-like phenotype. HSC activation leads to accumulation of scar (fibrillar) ECM. The presence of a fibrillar ECM in the Disse space has consequences for hepatocyte function, leading to the loss of microvilli and endothelial fenestrae. Therefore, the loss of normal tissue architecture contributes to impairment of organ function.

Etiology of liver fibrosis

The main causes of fibrosis are HCV infection and alcoholic liver disease, which account for more than half of cases [10]. Other major causes are hepatitis B virus (HBV) infection;

autoimmune hepatitis; chronic cholestasis, namely primary biliary cirrhosis and primary sclerosing cholangitis; and genetic metabolic diseases (hemochromatosis and Wilson disease). Due to the current epidemics of obesity, NASH is increasingly recognized as a major cause of fibrosis, yet its actual prevalence is still unknown.

1.2 Pathophysiologic Relevance of Cytokines in Chronic Liver Disease

Liver fibrogenesis is believed to be mediated to a great extent via complex interactions between liver parenchymal and nonparenchymal cells and involves increased production of cytokines. There is increasing evidence that several cytokines (TGF- β , Interleukin-1, Interleukin-6, Interleukin-8), mediate hepatic inflammation, apoptosis and necrosis of liver cells, cholestasis, and fibrosis, but paradoxically, they also mediate the regeneration of liver tissue after injury [2], [16], (Fig.2).

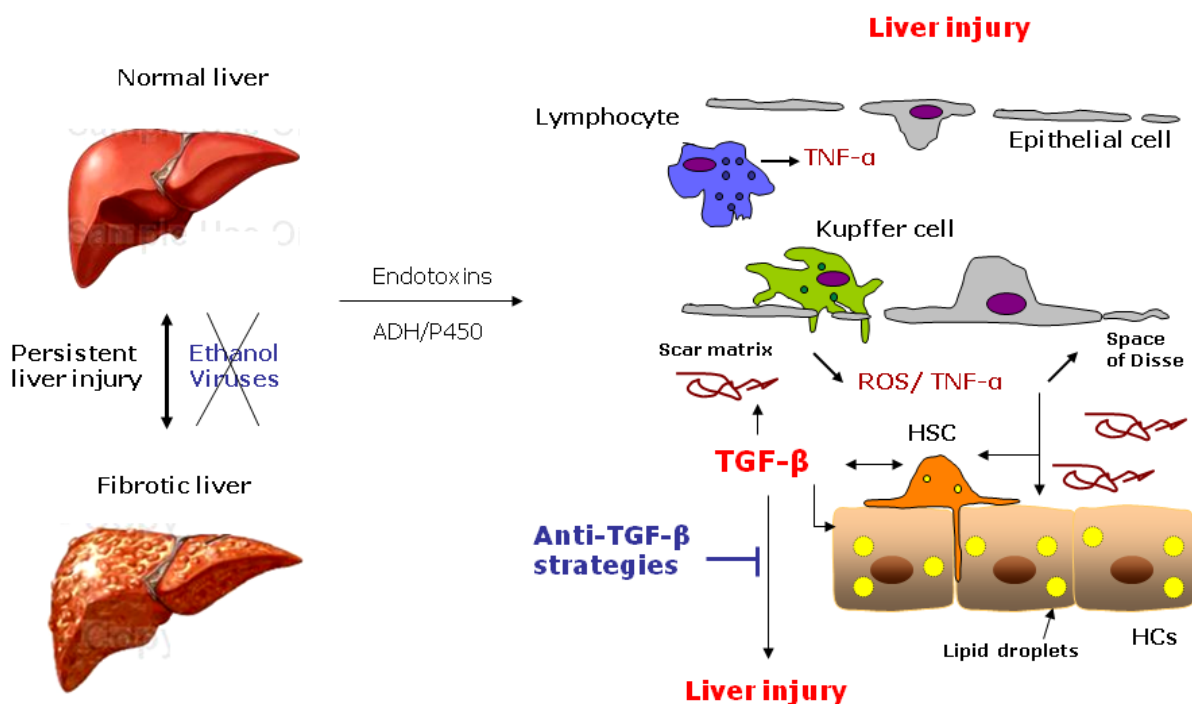


Fig. 2 Pathophysiologic Relevance of Cytokines in Chronic Liver Disease. Most types of cells in the liver, including Kupffer cells, hepatocytes, and stellate cells, either synthesize or respond to cytokines. In the early phase of chronic liver disease, specific agents such as viruses, ethanol, and toxins may stimulate the production of cytokines. In the late phase, endotoxin may be the key agent stimulating cytokine production. Clinical features of chronic liver disease that are mediated by cytokines include cachexia, cholestasis, fibrosis, synthesis of acute-phase proteins, and hypergammaglobulinemia. Whereas proinflammatory cytokines such as tumor

necrosis factor α (TNF α) and interleukin-6 are mainly involved in cholestasis and the synthesis of acute-phase proteins, transforming growth factor β (TGF β) released by activated Kupffer cells and hepatocytes may be one of the critical cytokines involved in fibrosis. In patients with progressive liver disease, the balance between proinflammatory and antiinflammatory cytokines may be shifted toward the proinflammatory axis, thus the counteracting anti-inflammatory cytokines are unable to control inflammation and fibrosis. www.doereport.com/generateexhibit.php?ID=13003

1.3 TGF- β in fibrogenesis

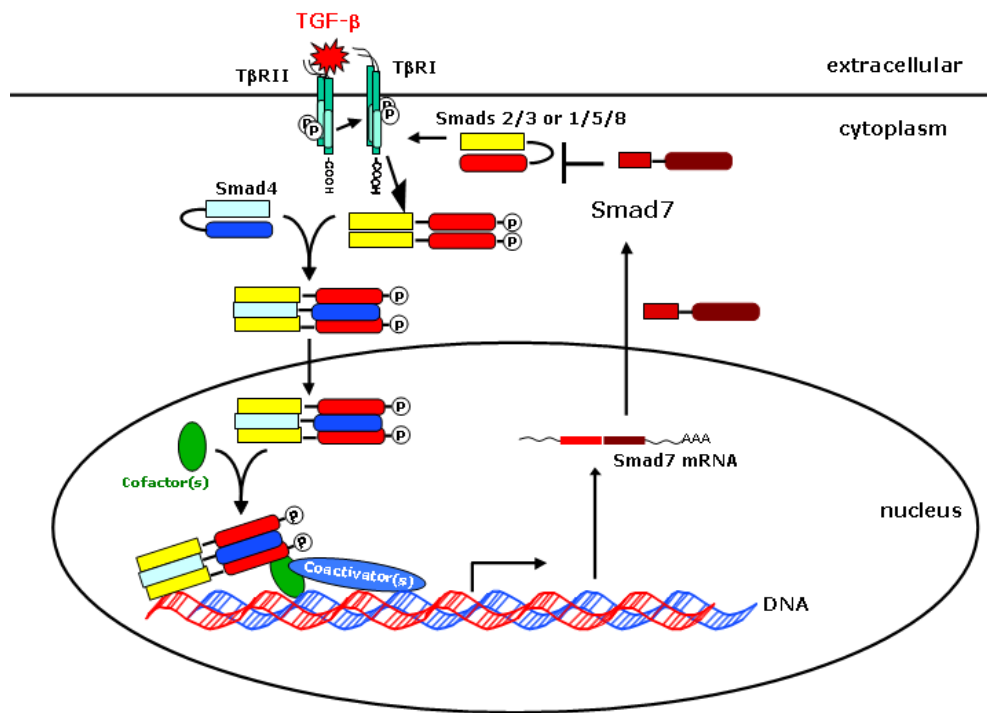
TGF- β is produced by a lot of liver cells during acute and chronic damage, e.g. Kupffer cells (KCs), hepatic stellate cells (HSCs), lymphocytes [18]. By activating canonical downstream Smads protein, TGF- β promotes quiescent HSCs transdifferentiating into myofibroblasts (MFBs) and induces MFBs to produce extracellular matrix (ECM). More recently, works from other groups and us demonstrate that TGF- β leads to epithelial-mesenchymal transition (EMT) of hepatocytes, thus contributing to liver fibrogenesis [4], [19].

It is suggested that repeated injury with continued autoinduction of TGF- β overrides the normal termination signals, thus creating a chronic vicious circle of TGF- β overproduction [14].

1.4 TGF- β signal transduction

TGF- β 1 belongs to a family of cytokines, which includes three isoforms of TGF- β , activins and bone morphogenic proteins (BMPs) [57].

The initial step bases on binding of the ligand and induction of the formation of heteromeric complexes composed of specific type I and type II receptor serin/threonin kinases on the cell surface [12]. In this complex constitutively phosphorylated receptor type II phosphorylates receptor type I at a highly conserved intracellular domain called GS domain [9]. The TGF- β family of receptors includes five receptors type II and seven receptors type I, which differ in their affinities to specific ligands, as well as in the choice of Smads, specific intracellular molecules, triggering a diversity of cellular responses (**Fig. 3**).



(Modified from Dooley et al., 2006)

Figure 3: Schematic representation of the Smad signaling cascade downstream of the TGF- β receptors. Initiation of signaling occurs when TGF- β binds to the serine/threonine kinase known as T β RII. Ligand-bound T β RII interacts with and phosphorylates the transducer receptor, T β RI. Activated T β RI then recruits and phosphorylates R-Smads, which associate to Co-Smad4. The heterocomplex translocates into the nucleus where it acts as a transcriptional regulator of target genes [6]. Smad7 blocks the TGF- β signal cascade on the level of R-Smad phosphorylation.

Negative regulators of the TGF- β signaling: Smad7

Signal termination is mediated by several mechanisms, like competitive binding of I-Smads (Smad6 or Smad7) with activated TGF- β receptors, ubiquitination and proteasome-mediated degradation of the TGF- β receptors and R-Smads [12]. On the basal state, I-Smads reside mainly in the nucleus, and upon TGF- β stimulation they are exported to the cytoplasm. Further, I-Smad expression is induced as response to TGF- β stimulation, thereby creating a negative feedback loop that leads to signal termination. Once in the cytoplasm, I-Smads bind to activated TGF- β receptors, resulting in signal termination via competing with R-Smads for receptor accessibility and mediating receptor degradation by facilitating their interaction with E3 ubiquitin ligases called Smurfs (Smad ubiquitination regulatory factors) 1 and 2, (Smurfs) [7], [12].

1.5 Animal models for liver disease

Several animal models for liver fibrosis have been established in the past and are still in use. Bile duct ligation (BDL) is a well established *in vivo* model to generate liver fibrogenesis based on cholestasis [5].

2. Aim of the study

The study presented here is based on previous work [5], where we succeeded in ameliorating fibrogenesis in BDL rats by injection of AdSmad7 via the portal/tail vein. Smad7-overexpression in rats with BDL displayed reduced collagen and α -SMA expression as well as decreased hydroxyproline content in the liver compared to animals treated with AdLacZ. A beneficial effect was even observed when Smad7 was expressed in animals with established fibrosis. In the present study, we were interested to investigate the effects of Smad7 overexpression specifically in smooth muscle cells. Therefore SM22 α -Flag-Smad7 mice transgenic mice expressing Smad7 under the control of the SM22 α promoter were generated for this purpose. As reference strains of FVB wild type were examined. Ectopic Smad7 expression was induced by activation of HSCs following bile duct ligation. The common bile duct was ligated twice and closed at the abdomen to induce fibrosis and transgenic Smad7 overexpression. The sham operation was performed without BDL. After 2 weeks, tissues were analyzed for the expression of fibrotic marker proteins. Sirius red staining was performed to assay collagen deposition and immunostaining was used to quantify the expression of α -SMA. Further, liver enzyme activities in the serum were measured.

Moreover, we analyzed Smad7 influence on HSC expression pattern in great detail using microarray analysis. Its overexpression influences a great variety of cellular pathways, involved in development, angiogenesis, differentiation, immune response, apoptosis, proliferation or signal transduction.

In summary, we demonstrated that overexpressed Smad7 inhibits HSC transdifferentiation and attenuates the extent of fibrosis suggesting a promising antifibrotic tool for treatment approaches.

3. Materials and Methods

3.1 Animals

All protocols for experiments with animals were carried out in full compliance with the guidelines for animal care and were approved by the Animal Care Committee from the government.

Generation of transgenic SM22 α -Flag-Smad7 mice: The targeting vector consisted of the murine SM22 α promotor (1,6 kb) followed by the Flag-Tag nucleotide sequence, a 1,3 kb-fragment containing the coding sequence of the murine Smad7 gene and a PGKneobpA as well as a β -lactamase expression cassette. The mice were used between 2 and 4 months of age. Over-expression of Smad7 in the transgenic mice was confirmed by measuring mRNA of Flag-Smad7 by PCR.

3.2 Establishing liver damage with bile duct ligation

Bile duct ligation was performed using a standard technique [5]. Briefly, FVB/N wild type and SM22 α -Flag-Smad7 transgenic mice (n=4 each group) were anesthetized by ketamine-kylazine. After midline laparotomy, the common bile duct was exposed and twice ligated with 6-0 silk suture. This model for *in vivo* studies generates liver fibrogenesis very efficiently based on cholestasis. Sham operation was performed by gently touching the bile duct. The abdomen was closed in layers, and the animals were allowed to recover on a heat pad. Animals were sacrificed 2 weeks after operation.

3.3 Detection of mRNA expression

Total RNA was collected from three (3d-) or seven days old (7d-) HSCs, which were either infected with AdSmad7, AdLacZ two days earlier or were uninfected. RNA isolation was performed using the RNeasy kit (Qiagen, Hilden, Germany) according to the instruction manual.

Total RNA was purified from liver tissue after homogenization in TRIZOL reagent (GIBCO BRL, Eggenstein, Germany; 1 ml/50mg tissue) using an UltraTurrax (IKA, Staufen, Germany). Samples were normalized by total RNA measurements (260/280 nm) and RNA gel electrophoresis. Liver RNA samples from four animals were pooled and cDNA was prepared

using the One step RT-PCR Kit from Qiagen (Hilden, Germany).

Affymetrix gene chip array of cultured HSCs

To identify Smad7 dependent gene responses, HSCs were infected 2 days following seeding with adenoviruses encoding for LacZ control (AdLacZ) or Smad7.

RNA sample collection and generation of biotinylated complementary RNA probes was carried out according to the Affymetrix GeneChip® Expression Analysis Technical Manual (Affymetrix, Santa Clara, CA, USA). Purified cDNA was used to synthesize biotinylated complementary RNA using the BioArray High Yield RNA Transcription Labeling Kit (Enzo Diagnostics, Enzo Life Science Inc., Farmingdale, NY, USA). Each sample was hybridized to an Affymetrix rat Genome RG-U34A microarray (8,799 probe sets) for 16h at 45°C. Expression values of each probe set were determined and AdSmad7 infected samples were compared to AdLacZ infected controls using the Affymetrix Microarray Suite 5.0 software.

Intensities across multiple arrays were normalized to a target intensity of 2,500 using global normalization scaling. Genes whose expression levels were changed more than 2-fold ($p < 0.001$) in both experiments were considered to be significantly regulated by Smad7. These genes were investigated according to their molecular function and biological process by searching the gene ontology (GO) term database. Genes differentially expressed in AdSmad7 treated compared to controls were classified by “pathway” analysis (KEGG [<http://www.genome.jp/kegg/pathway.html>], PathwayArchitect, Stratagene).

3.4 Immunohistochemical staining

Liver specimens were fixed in 10% formalin and embedded in paraffin. Four-micrometer tissue sections were stained with H&E for routine examination or with picro-Sirius red for visualization of hepatic collagen deposition as described. All samples were scored simultaneously. Presented values were the mean of 10 fields (magnification 100X) taken from 5 liver sections per mouse. For SM22 α and α -SMA detection, a 1:300 dilution of a mouse monoclonal anti- α -SMA antibody and anti-SM22 α (Sigma) were used. Inflammation indices were quantified using immunostaining with antibodies to CD68 (diluted 1:75) and subsequent processing of the sections with a standard horseradish peroxidase– conjugated antibody system. Endogenous peroxidase was blocked with peroxidase blocking reagent (Dako) for 30 minutes. Slides were counterstained with aqueous Mayer’s Hämalaun (1.09249.2500; Merck, Darmstadt, Germany), and then immunopositive cells were counted. Quantification of histological stainings was performed either by morphometric analysis with Leica QWIN

software or calculating the relative number of positive cells (200 cells were evaluated per observation field). Presented values correspond to the means of 10 fields (magnification 100) taken from 5 liver sections per mouse of between 5 mice in total.

3.5 Serum Enzymes and Hepatic Fibrosis Indices

A total of 500 μ L blood was taken from anesthetized mice for liver enzyme serum values. Aspartate aminotransferase (AST), alanine aminotransferase (ALT), and alkaline phosphatase (AP) values were determined with Calibrator Kit3 (VITROS Chemistry Systems; Ortho-Clinical Diagnostics, Buckinghamshire, England). Concentration of total bilirubin was determined with a test kit (Corgenix, CO) at a wavelength of 450 nm using a Victor 1420 Multilable Counter spectrometer (Wallac, Wellesley, MA).

3.6 Statistical analysis

Results are expressed as means \pm SEM and were analyzed either by Mann–Whitney test or by analysis of variance followed by paired comparison when appropriate. Statistical analysis of quantitative RT-PCR data was performed with Student *t* test for paired data. A *P* value of <0.05 was regarded significant.

4. Results

4.1 Establishing liver damage with bile duct ligation and experimental design

Bile duct ligation in rodents is an experimental model for extrahepatic. BDL was performed using a standard technique [5]. FVB/N wild type and SM22 α –Flag-Smad7 transgenic mice (n=4 each group) were anesthetized by ketamine-kylazine. After midline laparotomy, the common bile duct was exposed and twice ligated with 6-0 silk suture. Sham operation was performed by gently touching the bile duct. The abdomen was closed in layers, and the animals were allowed to recover on a heat pad (**Fig. 4A**).

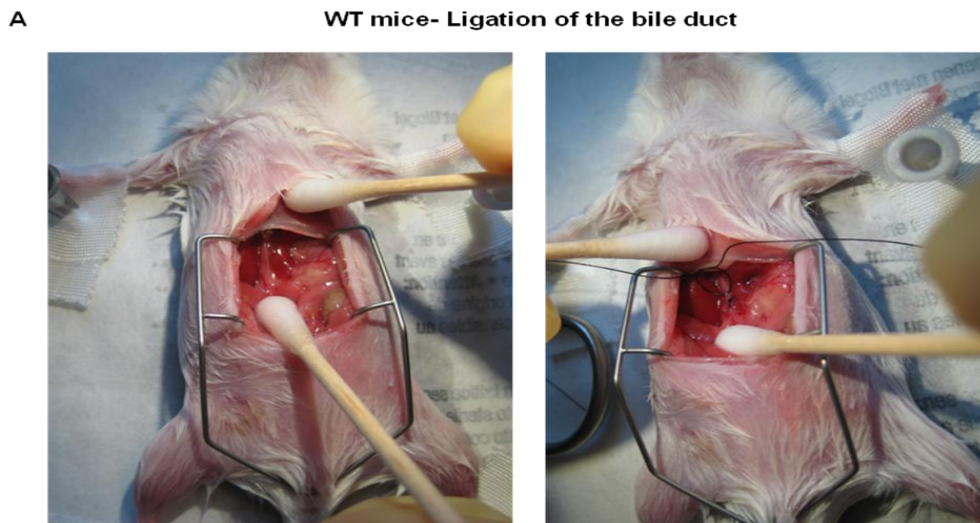


Figure 4. (A) *Establishing liver damage with bile duct ligation.* After midline laparotomy, the common bile duct was exposed and twice ligated with 6-0 silk suture.

Hepatic morphological abnormalities were examined in mice whose bile ducts had been irreversibly ligated for 14 days (**Fig. 4B**).

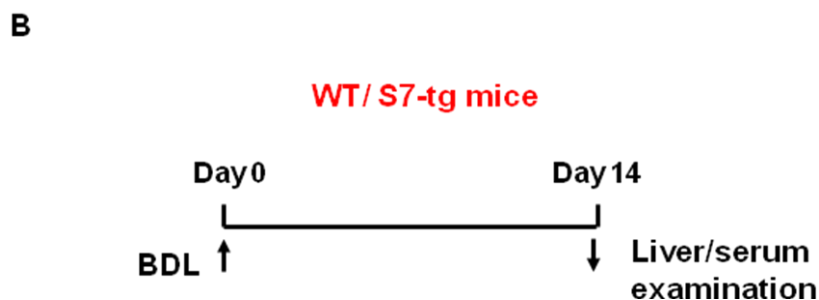


Figure 4. (B) *Experimental design.* The bile ducts from FVB/N wild type and SM22 α -Flag-Smad7 transgenic mice (n=4 each group) were ligated and the effect of HSCs-specific Smad7 expression on liver damage and fibrogenesis was analyzed after the mice were sacrificed at 2 weeks.

4.2 SM22 α -Flag-Smad7 expression in FVB/N and SM22 α -Flag-Smad7 transgenic after 2 weeks of BDL

In order to investigate the expression of Smad7 in transgenic mice PCR analysis was performed. Data showed that ectopic expression of Flag Smad7 mRNA was increased following 2 weeks of BDL in contrast to wild type animals. In FVB wild-type mice, BDL significantly induced TGF- β signaling, as determined by Col1 α 2 and α SMA mRNA

expression in liver tissue. The above indicators for fibrosis were significantly reduced in BDL-treated the SM22 α -Flag Smad7 mice after transgene induction. Smad7 mRNA levels remained unchanged in all the treatments groups (Fig.5).

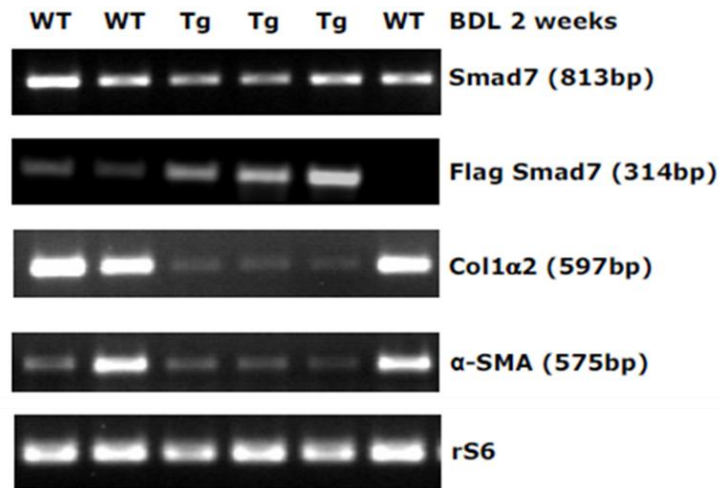


Figure 5. RT-PCR analysis to detect SM22 α -Flag Smad7 RNA expression. RT-PCR were performed to measure mRNA expression of Smad7, Flag-Smad7, col1 α 2, and α -SMA in liver tissues of wild type and SM22 α -Flag-Smad7 transgenic mice following 2 weeks of BDL.

4.3 Smad7 overexpression in HSCs decrease the serum levels of liver enzymes in BDL treated mice

Analysis showed that ALT levels increase rapidly with BDL induced liver damage in experimental control mice. After this medication FVB wild type mice produced approximately threefold more serum ALT (i.e. 570 ± 6.7 U/L) than SM22 α -Flag-Smad7 tg mice (i.e. 220 ± 3.7 U/L) ($p < 0.05$). A significant reduction of the ALT level in the serum of SM22 α -Flag-Smad7 tg mice can be observed in the BDL treated group. (Fig 6A).

In line with ALT levels indicating increased liver damage as a result of BDL induced fibrosis, AST concentrations are elevated after BDL treatment of wild-type mice compared with no BDL controls (i.e. 620 ± 6.1 U/L vs. 200 ± 2.5 U/L) ($p < 0.05$). Smad7 overexpression decreases serum levels of AST i.e. reduces the sensitivity for liver damage and fibrogenesis after BDL (**Fig 6B**). AP levels were measured to be 2400 ± 9.8 U/L BDL treatment and the resulting Smad7 overexpression causes the reduction of AP levels in SM22 α -Flag-Smad7 tg mice to 181.5 ± 11.5 (U/L). in comparison to wild-type mice (**Fig 6C**). Analysis showed that total bilirubin levels increase rapidly with BDL induced liver damage in FVB (i.e 10 mg/dl) mice compared with sham operated group (0.510 mg/dl) ($p < 0.05$). A significant reduction of the bilirubin level in the serum of SM22 α -Flag-Smad7 tg mice can be observed in the BDL treated group as compared with BDL treated FVB mice (**Fig 6D**).

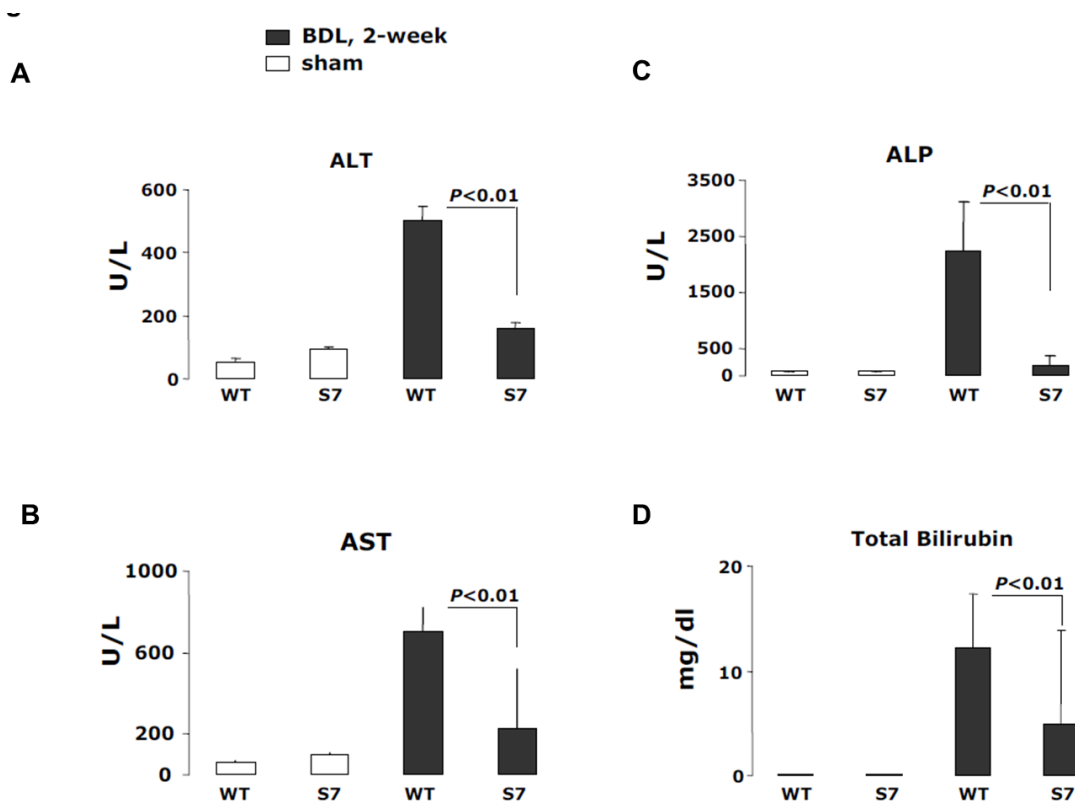


Figure 6. SM22 α -Flag-Smad7 transgenic mice improved liver fibrogenesis in 2 weeks of BDL model. Routine liver function indices, including (A) ALT, (B) AST, (C) ALP, and total bilirubin, showed in serum from wild type and SM22 α -Flag-Smad7 transgenic mice. Specific enzyme serum concentrations were measured at 400 nm with VITROS Chemistry Products; n, number of animals investigated in triplicate measurements (n=4).

4.4 Smad7 overexpression in HSCs decreases collagen deposition in BDL treated mice

Sirius red staining of liver sections from BDL wild-type mice demonstrated typical perisinusoidal, periportal, and peribiliary fibrosis, resulting in the formation of fibrotic septae as compared with sham operated group (**Fig. 7A**). The quantitative analysis of collagen content in liver sections from SM22 α -Flag-Smad7 tg BDL operated mice showed a significant resolution of perisinusoidal fibrosis, resulting in disappearance of fibrotic septae, however, deposition of ECM was still observed in periportal and peribiliary areas. (**Fig. 7B**). In the LPS treated group. No noticeable difference between collagen expression in FVB wild type and SM22 α -Flag-Smad7 S7tg mice could be detected in sham operated groups.

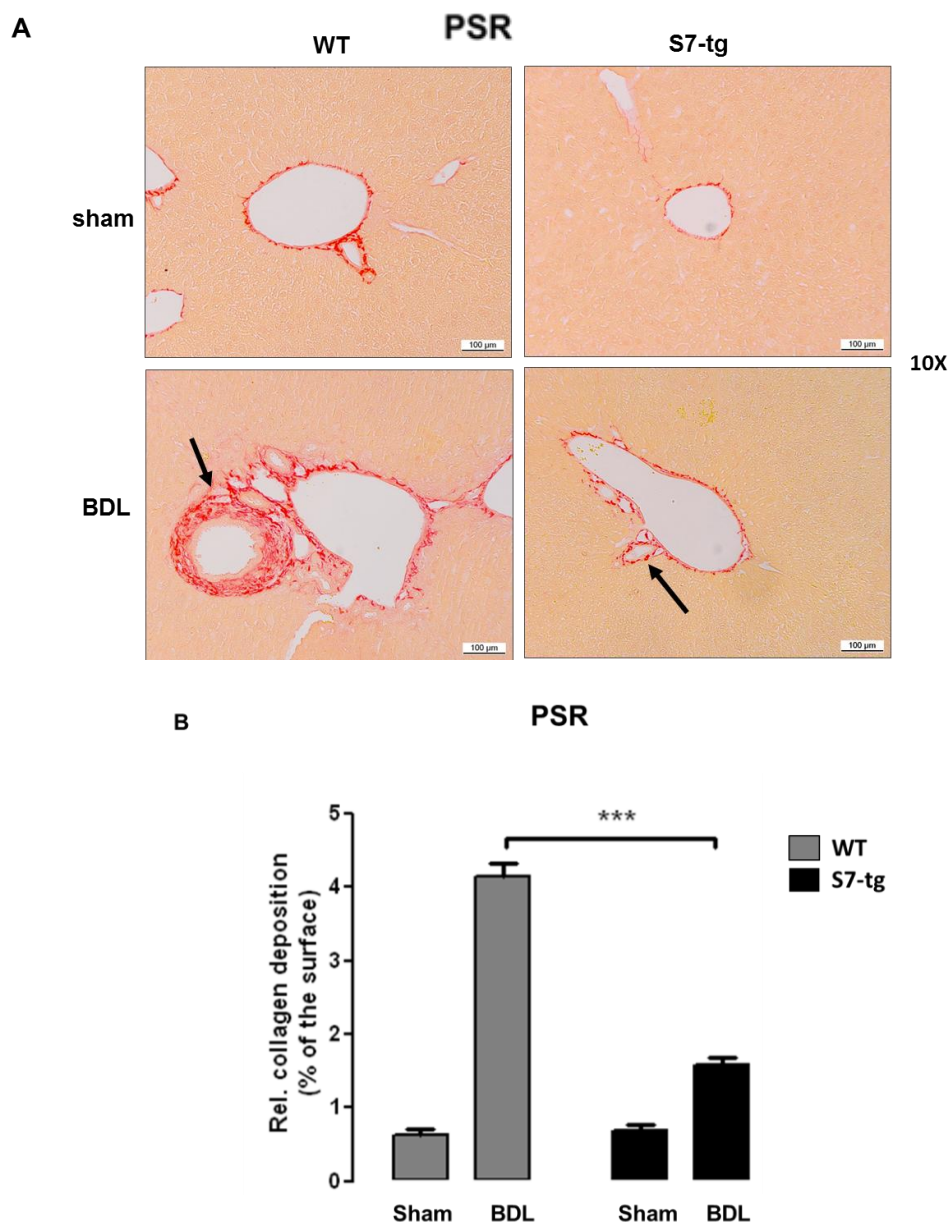
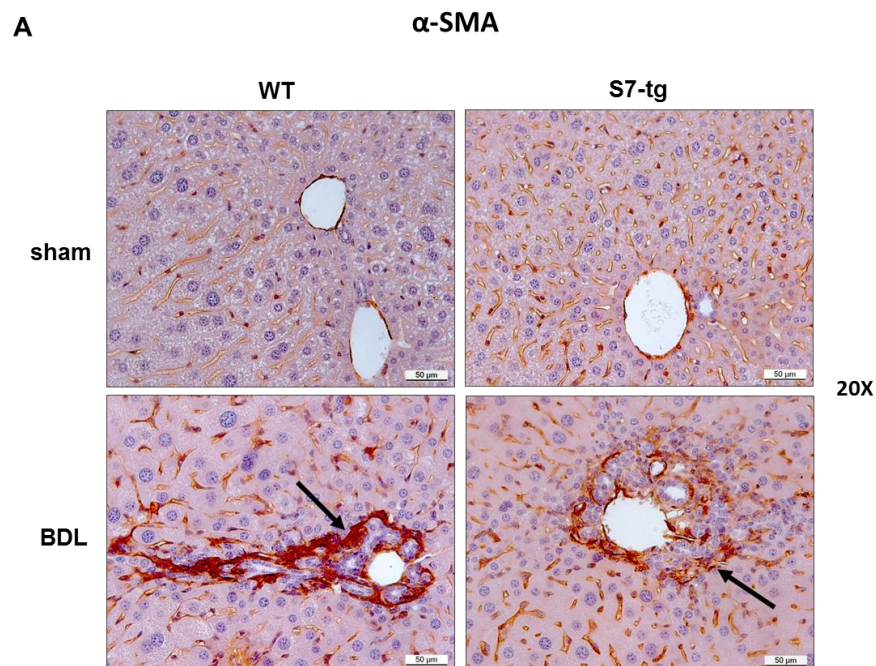


Figure 7. Smad7 overexpression decreases collagen deposition in BDL operated treated mice. (A) Representative photomicrographs of mice liver sections from SM22 α -Flag-Smad7 tg and FVB wild type animals 2 weeks following BDL or sham operated. Sirius red staining was performed to measure collagen deposition; magnification x 15. (B) Morphometric quantification of immunohistochemical staining of type I collagen was carried out by selecting ten fields randomly from each section of different groups (n=4/ group); LEICA QWIN software (Germany) was used. The graph shows the percentage of positive staining related to the total area investigated.

4.5 Smad7-overexpression leads to a decrease of α -SMA synthesis in liver cells of BDL treated mice.

α -SMA, positive cells were markedly decreased in SM22 α -Flag-Smad7 transgenic mouse compared with wild types after 2-weeks of BDL operation (**Fig.8A**). In conclusion, the morphometric analysis showed that the reduction of α -SMA synthesis is attributed to an inhibition of HSC activation, due to ectopic Smad7 overexpression (**Fig.8B**).



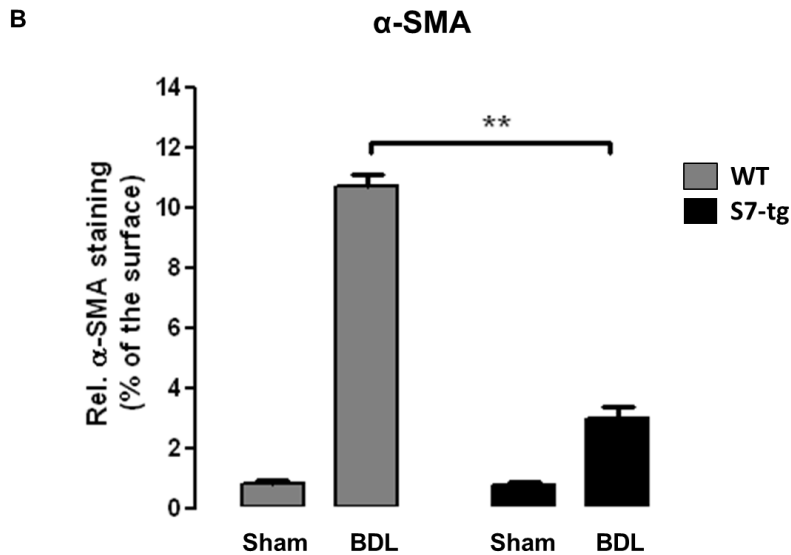


Figure 8. Smad7-overexpression leads to a decrease of αSMA synthesis in liver cells of BDL operated mice. (A) Immunohistochemical staining of αSMA as a marker for activated HSCs. Representative photomicrographs of mice liver sections from SM22α-Flag Smad7 tg and FVB wild type strains following 2 weeks of BDL or sham operated; magnification x 15. (B) Morphometric quantification of immunohistochemical staining of αSMA Ten fields were selected randomly from each section of different groups (n=4/ group); LEICA QWIN software (Germany) was used. The graph shows the percentage of stained areas related to the total area investigated.

4.6 Smad7 overexpression in HSCs blunts inflammation in BDL operated mice.

In order to determine the effect of Smad7 overproduction in HSCs on inflammations, an accompanying symptom of fibrosis, immunohistochemical staining with anti-CD68 antibodies was performed. The analysis indicates that BDL operated wild-type mice showed increase number of infiltrating macrophages as compared with sham operated group. Concomitant with decreased expression of fibrotic markers (α-SMA) CD68 marked Kupffer cells were significantly reduced in Smad7 transgenic mice compared with wild type mice following 2 weeks of BDL (**Fig.9A**). The morphometric analysis confirms that Smad7 overexpression in HSCs hepatocytes can inhibit BDL induced liver fibrosis and blunts the inflammatory state of the liver of those animals (**Fig.9B**).

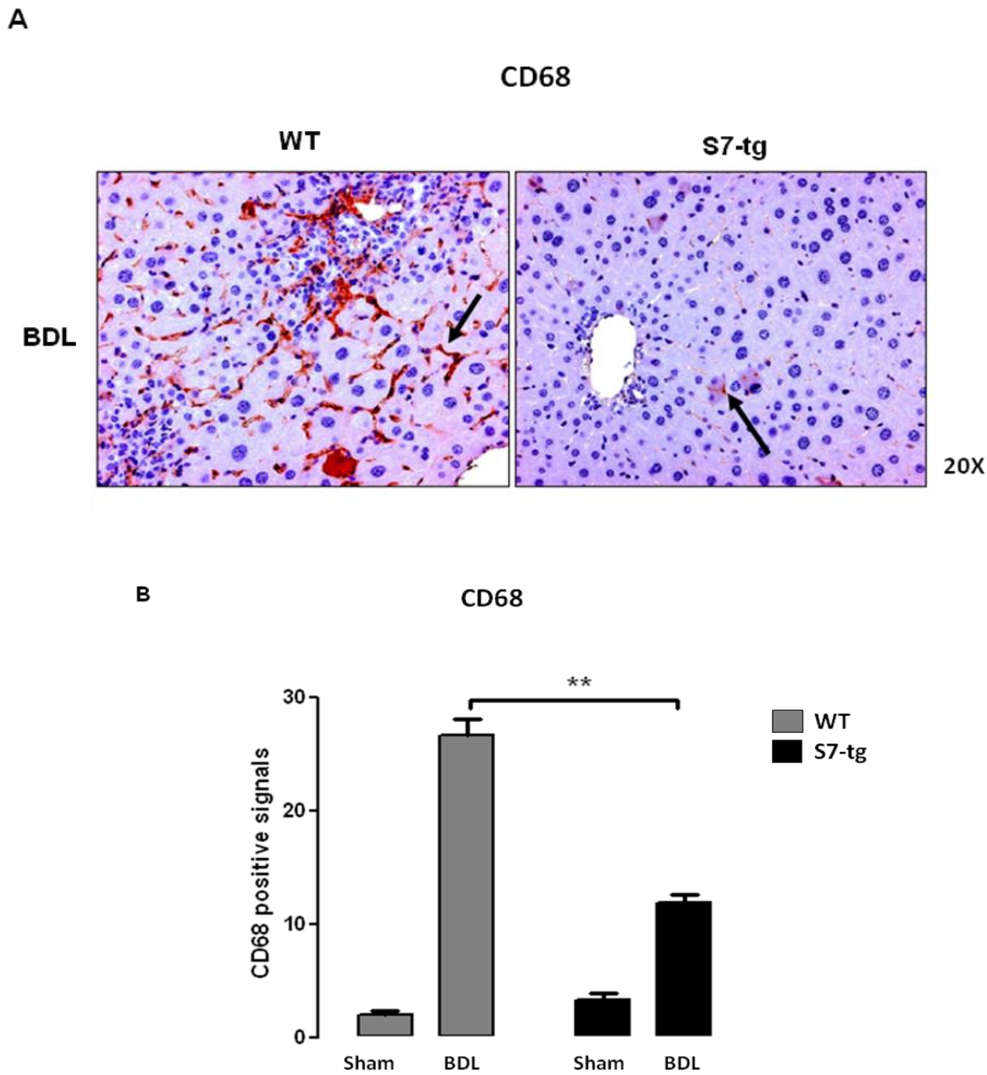


Figure 9. Smad7 overexpression leads to a blockade of TGF- β signaling and a decrease of inflammation after BDL induced liver damage. (A) Immunohistochemical staining of CD68 as a marker for activated macrophages. Representative photomicrographs of mice liver sections from SM22 α -Flag Smad7 tg and FVB wild type strains following 2 weeks of BDL or sham operated; magnification x 15. (B) Morphometric quantification of immunohistochemical staining for CD68. Ten fields were selected randomly from each section of different groups (n=4/ group); LEICA QWIN software (Germany) was used. The graph shows the levels of positive stained cells per field.

4.7 Smad7 dependent gene expression pattern

Primary rat HSCs were infected with AdSmad7 or AdLacZ (control). Transdifferentiating (3 d in culture) and fully activated (7 d in culture) HSCs were investigated. The expression of genes displayed on 8799 probe sets was compared between cells overexpressing Smad7 and

controls. In general, many known mediators of TGF- β signaling were differentially expressed in AdSmad7 infected HSCs, confirming a direct link of Smad7 effects to TGF- β signalling.

To validate our microarray results, we selected 12 genes from array data identified as highly regulated in dependency to Smad7 for RT-qPCR analysis. TGF- β RI mRNA expression is not modulated during transdifferentiation, and was used as the expression reference. A synopsis of Smad7 associated modulation of gene expression, given in **Fig.10** as log₂ fold of LacZ, generally supports the array results. We confirmed upregulation of Cyp4B1, BMP2, SGIII, Zfp423, Pla2g2a and downregulation of EST189231, Olr1 and Id1 independent of time during the transdifferentiation process (**Fig.10A, B**).

Interestingly, when comparing 3 d- with 7 d-HSCs, opposite effects of Smad7 were found for HK2 (0.38-fold in 3 d-, 3.85-fold in 7 d-HSCs), Slc16a3 (0.59-fold in 3 d, 2.25-fold in 7 d-HSCs) and VEGF.1 (0.51-fold in 3 d-, 1.07-fold in 7 d-HSCs), underlining temporal differences and modulation of the TGF- β signal during HSC activation.

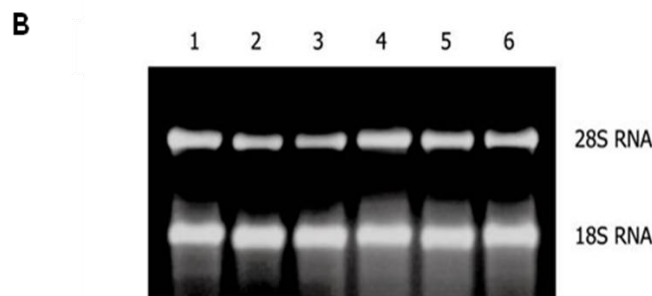
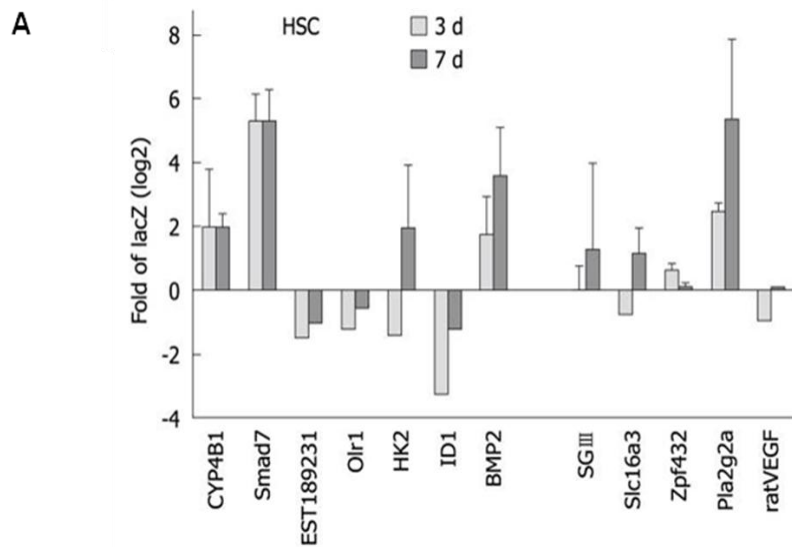


Figure 10. Validation of microarray results using quantitative real-time polymerase chain reaction. A: SYBR Green I-based real-time quantification to compare the mRNA expression patterns of 12 selected genes in hepatic stellate cell which were infected either with AdLacZ or AdSmad7. Transforming growth factor- β RI, not affected by Smad7 overexpression, served as a house-keeping gene. Results are given as relative expression of log₂ fold of LacZ. 3 d (light grey column) and 7 d (dark grey column): 3 d and 7 d after adenoviral infection. Values are the mean of three measurements each performed in duplicates \pm SD from independent experiments; B: Total RNA purity and integrity was verified by formaldehyde agarose gel electrophoresis. Lane 1: LacZ, 7 d; Lane 2: LacZ, 3 d; Lane 3: Smad7, 7 d; Lane 4: Smad 7, 3 d; Lane 5: Untreated control, 7 d; Lane 6: Untreated control, 3 d.

Glucose metabolism and angiogenesis/vascularisation is downregulated by Smad7

Hk2 is a hexokinase, one of the best known enzymes of glycolysis, and is involved in cell cycle progression. According to the results of the microarray analysis it represents the most downregulated gene in AdSmad7 infected HSCs. One feature of activated HSCs is the ability to proliferate. TGF- β antagonizes proliferation in quiescent HSCs, whereas it has a growth promoting effect in transdifferentiated MFBs. Thus, Hk2 might be induced by TGF- β in HSCs during activation, subsequently stimulating HSC proliferation and thus providing at least part of the growth stimulatory effect of TGF- β . Upregulation of Hk2 during activation of HSCs further suggests that glycolysis induction and increased levels of involved proteins may occur by other means than elevated blood glucose levels. This in turn indicates a direct connection between fibrosis and enhanced glycolysis independent of inducing external stimuli of either process (**Fig.11**).

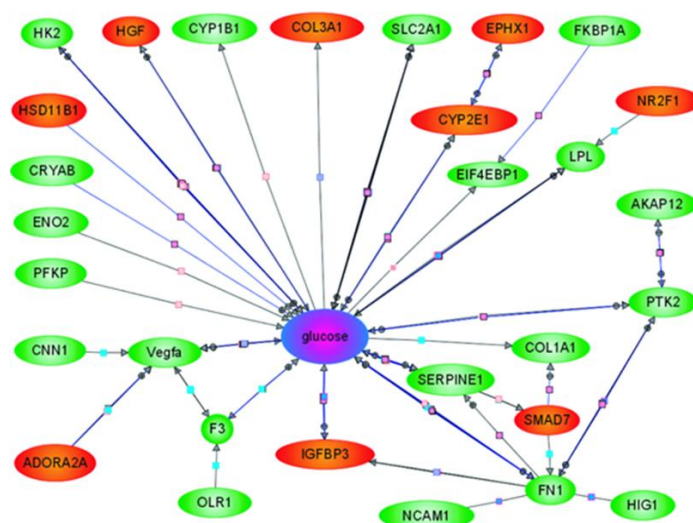


Figure 11 Biological interaction between glucose and genes up- (light grey) or down-regulated (white) in primary hepatic stellate cells after overexpression of Smad7. Genes linked to glucose by binding or

regulatory interactions are depicted as interconnecting lines between glucose and the gene symbols. Pathway analysis was done with Pathway Architect software (Stratagene).

5. Discussion

5.1 Myofibroblasts are the primary target of anti-fibrotic therapy

Liver myofibroblasts represent a primary target for anti-fibrotic therapy. In the fibrotic liver, hepatic stellate cells (HSCs) have been reported to contribute with >80% of the collagen producing cells [1]. Therefore, HSCs are currently considered to be the major, but not the only, source of myofibroblasts in the injured liver [1]. Although HSC death by apoptosis and senescence during the regression of liver fibrosis is well documented, its quantitative contribution is unknown [15]. TGF- β hyperactivity is recognized as the driving force of the fibrogenic response to injury and anti-TGF- β strategies were successfully used to counteract this process in different tissues, including liver, lung, and kidney [3]. Smad7 is a major inhibitory regulator of TGF- β superfamily signal transduction, and recent studies have implicated Smad7 as an important molecule for regulating TGF- β activity in human and experimental disease. Two recent approaches used adenoviral infection and overexpression of Smad7 to intervene profibrogenic TGF- β effects in vivo. Intratracheal injection of AdSmad7 was able to block bleomycin dependent Smad2 phosphorylation, resulting in suppression of collagen I mRNA, reduced hydroxyproline content, and missing fibrotic responses in the lungs, suggesting that Smad7 may have the potential to treat pulmonary fibrosis.

Previous publications concluded that Smad7 overexpression completely inhibits autocrine and paracrine TGF- β signaling in HSCs, leading to abrogation of Smad2/3 activation and subsequent downstream events. Our results further indicate that HSCs remained in a quiescent stage after Smad7 overexpression confirming the important role of TGF- β signaling during the early phase of HSC activation.

Therefore SM22 α -Flag-Smad7 mice transgenic mice expressing Smad7 under the control of the SM22 α promoter were generated for this purpose. In SM22 α -Flag-Smad7 tg mice the Smad7 gene was expressed under the control of the human SM22 α promoter. Ectopic Smad7 expression was induced by activation of HSCs following bile duct ligation. As reference strains of FVB wild type were examined. The common bile duct was ligated twice and closed

at the abdomen to induce fibrosis and transgenic Smad7 overexpression. The sham operation was performed without BDL. After 2 weeks, tissues were analyzed for the expression of fibrotic marker proteins. Sirius red staining was performed to assay collagen deposition and immunostaining was used to quantify the expression of α -SMA. Further, liver enzyme activities in the serum were measured.

Our data showed that ectopic expression of Flag Smad7 mRNA was increased following 2 weeks of BDL in contrast to wild type animals. In FVB wild-type mice, BDL significantly induced TGF- β signaling, as determined by Col1 α 2 and α SMA mRNA expression in liver tissue. The above indicators for fibrosis were significantly reduced in BDL-treated the SM22 α -Flag Smad7 mice after transgene induction.

Analysis of serum levels of liver enzymes reveals important parameters of the state of liver fibrosis. As expected, AST and ALT, total bilirubin and alkaline phosphatase (AP) serum levels show significant increase in SM22 α -Flag-Smad7 tg mice BDL operated when compared to wild-type mice. Smad7 overexpression causes the reduction of all above serum biomarkers in BDL operated mice. These results can be interpreted to be due to antifibrotic effects of Smad7 overexpression interrupting the TGF- β signaling pathway in HSCs.

Collagen is one of main the components of the ECM produced by activated HSC in damaged tissues [10]. Sirius red staining of liver sections from BDL wild-type mice demonstrated typical perisinusoidal, periportal, and peribiliary fibrosis, resulting in the formation of fibrotic septae as compared with sham operated group. The quantitative analysis of collagen content in liver sections from SM22 α -Flag-Smad7 tg BDL operated mice showed a significant resolution of perisinusoidal fibrosis, resulting in disappearance of fibrotic septae, however, deposition of ECM was still observed in periportal and peribiliary areas.

Finally, the rate of inflammation, usually accompanying liver fibrosis, in dependency of HSCs specific Smad7 expression was examined. TGF- β is described as one of the most potent inducers of apoptosis in normal hepatocytes [6]. Immunohistochemical staining with anti-CD68 antibodies points to a dramatic reduction of inflammation in livers of SM22 α -Flag-Smad7 tg mice BDL operated, in parallel with a decrease of detectable fibrosis. Similarly, overexpression of Smad7 in kidney inhibits renal inflammation in remnant kidney disease [6].

5.2 The influence of Smad7, antagonist of transforming growth factor (TGF)- β canonical signaling pathways on hepatic stellate cell (HSC) transdifferentiation

To analyse the effects of Smad7 overexpression during HSC transdifferentiation we used Affymetrix Microarray approach. All gene expression changes found constitute potential starting points for future research projects to unravel the process of liver fibrogenesis.

5.3 Glucose metabolism and angiogenesis/vascularisation is downregulated by Smad7

Hk2 is a hexokinase, one of the best known enzymes of glycolysis, and is involved in cell cycle progression. According to the results of the microarray analysis it represents the most downregulated gene in AdSmad7 infected HSCs. One feature of activated HSCs is the ability to proliferate. TGF- β antagonizes proliferation in quiescent HSCs, whereas it has a growth promoting effect in transdifferentiated MFBS. Thus, Hk2 might be induced by TGF- β in HSCs during activation, subsequently stimulating HSC proliferation and thus providing at least part of the growth stimulatory effect of TGF- β . Although physiological effects of glucose metabolism in the liver are traditionally associated to hepatocytes and provide a direct link to fibrogenesis *via* hyperglycemia and insulin resistance [14], one could speculate that activated HSCs need more energy and thus, glycolysis is upregulated TGF- β dependently in this cell type. In line, HSCs become sensitive to glucose signaling during activation, high glucose concentrations stimulate ROS production through PKC-dependent activation of NADPH oxidase and induce MAP kinase phosphorylation subsequent to proliferation and type I collagen production in this cell type suggesting a crucial role of HSC-sugar metabolism in fibrogenesis [15].

Upregulation of Hk2 during activation of HSCs further suggests that glycolysis induction and increased levels of involved proteins may occur by other means than elevated blood glucose levels. This in turn indicates a direct connection between fibrosis and enhanced glycolysis independent of inducing external stimuli of either process.

6. Conclusions

Taken together, the data demonstrates that TGF- β signaling in HSCs is required for progression of chronic liver disease and blocking its signaling pathway in this cell type by ectopic expression of Smad7 is sufficient to obtain a beneficial outcome. In vivo data demonstrated that overexpressed Smad7 inhibits HSC transdifferentiation and attenuates the extent of fibrosis suggesting a promising antifibrotic tool for treatment approaches.

7. Keywords

TGF- β , Smad7, fibrosis, bile duct ligation, liver

8. References

1. Bataller R, Brenner DA (2005) Liver fibrosis. *J Clin Invest* 115:209–218
2. De Minicis S, Seki E, Uchinami H, Kluwe J, Zhang Y, Brenner DA, Schwabe RF. Gene expression profiles during hepatic stellate cell activation in culture and in vivo. *Gastroenterology*. 2007;132:1937–1946
3. Dooley S, Streckert M, Delvoux B, Gressner AM (2001b) Expression of Smads during in vitro transdifferentiation of hepatic stellate cells to myofibroblasts. *Biochem Biophys Res Commun* 283:554–562
4. Dooley S, Hamzavi J, Breitkopf K, Wiercinska E, Said HM, Lorenzen J, Dijke ten P, Gressner AM (2003) Smad7 prevents activation of hepatic stellate cells and liver fibrosis in rats. *Gastroenterology* 125:178–191
5. Dooley S, Hamzavi J, Ciuculan L, Godoy P, Ilkavets I, Ehnert S, Ueberham E, Gebhardt R, Kanzler S, Geier A, Breitkopf K, Weng H, Mertens PR (2008) Hepatocyte-specific Smad7 expression attenuates TGF- β -mediated fibrogenesis and protects against liver damage. *Gastroenterology* 135:642–659
6. Dooley S, Weng H, Mertens PR (2009) Hypotheses on the role of transforming growth factor- β in the onset and progression of hepatocellular carcinoma. *Dig Dis* 27:93–101

7. Friedman SL (2010) Evolving challenges in hepatic fibrosis. *Nat Rev Gastroenterol Hepatol* 7:425–436
8. Iredale JP (2007) Models of liver fibrosis: exploring the dynamic nature of inflammation and repair in a solid organ. *J Clin Investig* 117:539–548
9. Iyer S, Wang ZG, Akhtari M, Zhao W, Seth P (2005) Targeting TGF β signaling for cancer therapy. *Cancer Biol Ther* 4:261–266
10. George J, Roulot D, Koteliensky VE, Bissell DM (1999) In vivo inhibition of rat stellate cell activation by soluble transforming growth factor β type II receptor: a potential new therapy for hepatic fibrosis. *Proc Natl Acad Sci USA* 96:12719–12724
11. Giannelli G, Mazzocca A, Fransvea E, Lahn M, Antonaci S (2011) Inhibiting TGF- β signaling in hepatocellular carcinoma. *Biochim Biophys Acta* 1815:214–223
12. Liu C, Gaca MD, Swenson ES, Vellucci VF, Reiss M, Wells RG (2003) Smads 2 and 3 are differentially activated by transforming growth factor- β (TGF- β) in quiescent and activated hepatic stellate cells. Constitutive nuclear localization of Smads in activated cells is TGF- β -independent. *J Biol Chem* 278:11721–11728
13. Michalopoulos GK (2011) Liver regeneration: alternative epithelial pathways. *Int J Biochem Cell Biol* 43:173–179
14. Parekh S, Anania FA. Abnormal lipid and glucose metabolism in obesity: implications for nonalcoholic fatty liver disease. *Gastroenterology*. 2007;132:2191–2207.
15. Sugimoto R, Enjoji M, Kohjima M, Tsuruta S, Fukushima M, Iwao M, Sonta T, Kotoh K, Inoguchi T, Nakamura M. High glucose stimulates hepatic stellate cells to proliferate and to produce collagen through free radical production and activation of mitogen-activated protein kinase. *Liver Int*. 2005;25:1018–1026.
16. Tahashi Y, Matsuzaki K, Date M, Yoshida K, Furukawa F, Sugano Y, Matsushita M, Himeno Y, Inagaki Y, Inoue K (2002) Differential regulation of TGF- β signal in hepatic stellate cells between acute and chronic rat liver injury. *Hepatology* 35:49–61
17. Taura K, Miura K, Iwaisako K, Osterreicher CH, Kodama Y, Penz-Osterreicher M, Brenner DA (2010) Hepatocytes do not undergo epithelial-mesenchymal transition in liver fibrosis in mice. *Hepatology* 51:1027–1036
18. Wynn TA (2004) Fibrotic disease and the T(H)1/T(H)2 paradigm. *Nat Rev Immunol* 4:583–594
19. Zeeberg BR, Feng W, Wang G, Wang MD, Fojo AT, Sunshine M, Narasimhan S, Kane DW, Reinhold WC, Lababidi S, et al. GoMiner: a resource for biological interpretation of genomic and proteomic data. *Genome Biol*. 2003;4:R28.